Narrowband lamellar multilayer grating with low contrast $MoSi_2$/Si materials for soft X-ray region

Qiushi Huang[1], Jiangtao Feng[1], Tongzhou Li[1], Xiangmei Wang[1], Igor V. Kozhenikov[2], Yang Yang[1], Runze Qi[1], Andrey Sokolov[3], Mewael Giday Sertsu[3], Franz Schäfers[3], Wenbin Li[1], Chun Xie[4], Zhong Zhang[1] and Zhanshan Wang[1,*]

[1] *Key Laboratory of Advanced Micro-Structured Materials MOE, Institute of Precision Optical Engineering, School of Physics Science and Engineering, Tongji University, Shanghai 200092, China*
[2] *Shubnikov Institute of Crystallography of Federal Scientific Research Centre "Crystallography and Photonics" of the Russian Academy of Sciences, Leninskiy pr. 59, Moscow 119333, Russia*
[3] *Helmholtz-Zentrum Berlin für Materialien und Energie, BESSY-II, Albert-Einstein-Str. 15, 12489 Berlin, Germany*
[4] *Sino-German College of Applied Sciences, Tongji University, 200092, Shanghai, China*
**Corresponding author: wangzs@tongji.edu.cn*

Abstract

To develop highly efficient narrow-bandwidth multilayer optics for the soft X-ray (SXR) spectroscopy, a low optical contrast $MoSi_2$/Si lamellar multilayer grating (LMG) was proposed and developed. The low contrast LMG allows for a large lamel width which can potentially achieve higher resolution than the conventional LMG and simplify the fabrication. As a first demonstration, a $MoSi_2$/Si multilayer with a d-spacing of 5 nm and 180 bilayers was deposited. The lamellar grating structure with a period of 614 nm, lamel-to-period ratio of 0.38, and lamel height of 670 nm was fabricated in the multilayer with reactive ion etching process. The SXR measurements show a high 0th-order diffraction efficiency of 16%–33% at 876 eV–1648 eV, which reaches around 80% of the unetched multilayer reflectivity. A maximal bandwidth reduction of 2.2 times was obtained compared with the multilayer mirror, indicating an energy resolution of $E/\Delta E = 108$ at 1183 eV. The resolution can be further improved by reducing the multilayer d-spacing and increasing the etching depth.

Keywords: lamellar grating, multilayer, X-ray, reflectance, bandwidth

1. Introduction

One-dimensional multilayer structures have long been used as mirrors for the soft X-ray (SXR) and extreme ultraviolet (EUV) ranges. They enable the reflection of SXR/EUV light above the total external reflection region (up to the normal incidence) and bring the advantages of large numerical apertures and high efficiency for high-resolution imaging [1] and manufacturing [2]. To extend their applicability, the one-dimensional multilayer mirror (MM) is combined with two-dimensional diffraction structures, such as the blazed multilayer grating [3,4] or lamellar multilayer grating (LMG) [5], or is sectioned directly to become a diffraction element, like the sliced multilayer grating and multilayer Laue Lens [6].

Deeply etched LMG, the structure of which can be seen in Fig. 1, provides more freedom for the bandwidth tuning of a multilayer. The bandwidth of a conventional MM is determined by the number of bilayers (N) contributing to the Bragg reflection, which is limited by X-ray absorption. The resolution ($E/\Delta E$) is typically around 50 in the SXR/EUV ranges [5], in which the absorptivity of all materials is high. However, X-ray fluorescence or other emission spectroscopy requires high-resolution dispersive optics to resolve close emission lines and their shapes for an elemental analysis or plasma diagnostics [7, 8]. Deep etching of grating structures into an MM decreases the X-ray absorption and increases the radiation penetration depth and LMG resolution. In the early works, LMGs based on different multilayer structures have been designed and fabricated for the energy range from B-K to Ar-K emission lines [9,10].

To further understand the diffraction behavior and optimal performance of the LMGs, Kozhevnikov et al. established a single-order operation regime for the LMGs [11,12], i.e. the incident wave excites only one diffraction wave and the 0^{th} order diffraction efficiency of an LMG can reach the peak reflectance of conventional MMs, whereas the reflectivity bandwidth $\Delta\theta$ is decreased by a factor of Γ

(the ratio of the lamel width to the grating period D). The necessary condition of the single-order regime is that the angular width of the diffraction peak $\Delta\theta = \Gamma\Delta\theta_{MM}$ is essentially narrower than the angular distance (in terms of the incidence angle) between neighboring diffraction peaks $\delta\theta \approx d/D$, where d is the MM period and $\Delta\theta_{MM}$ is the angular width of the initial MM. Thus, the necessary condition is written in the following form

$$\Gamma D\Delta\theta_{MM} \ll d, \quad (1)$$

More detailed discussion of Eq. (1) is given in [11, 12], where, the "much less" in Eq. (1) implies that the value is smaller by at least a factor of 3~5, depending on the spectral region. Note that condition (1) depends on the lamel width ΓD rather than on the grating period, which makes the lamel width a critical parameter in the fabrication of LMG. Based on the theoretical results obtained in [11,12], van der Meer et al. designed and fabricated high-aspect ratio W/Si LMGs [13] operating in the single-order regime, with the diffraction efficiency reached above 80% of the multilayer mirror reflectivity.

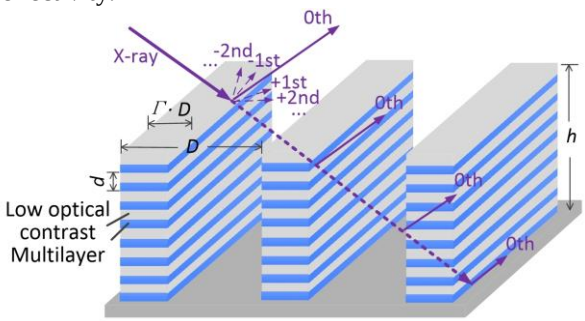

Fig. 1. Schematic of the low optical contrast LMG structure characterized by the grating period D and lamel width ΓD. The multilay inside each lamel has a period of d and a total thickness of h. The incident beam is diffracted into a set of waves by the grating. However, if the condition of the single-order regime (Eq. (1)) is fulfilled, only one diffraction wave, e.g., the 0^{th} order is effectively excited as depicted here.

An LMG design with a desired reflectivity bandwidth ΔE at photon energy E consists of several steps: (a) The materials and structure parameters of the initial MM are chosen in accordance with the principles described in [14] to achieve maximal reflectivity; (b) the grating ratio Γ is chosen considering the desired spectral resolution with $\Gamma = \Delta E/(\Delta E)_{MM}$, where ΔE and $(\Delta E)_{MM}$ is the spectral reflectivity bandwidth of the LMG and the initial MM, respectively; (c) the number of bilayers is increased by a factor of 1/ Γ compared with the initial MM; (d) the grating period D is chosen to realize condition (1) of the single-order regime. We note that the LMG resolution is independent of the chosen material pair of the MM. This is because the single-order LMG can be considered as a conventional MM with the density of both materials decreased by the factor Γ [11,12]. Hence, theoretically speaking, the optical contrast between neighboring layers can be reduced to any desired value independent of the real LMG materials. Previous works on LMG mainly choose conventional high optical contrast materials for the multilayer.

However, there are technical limitations imposed by the current fabrication technology on the geometrical parameters and possible material pairs of the LMGs. Indeed, the angular bandwidth of a conventional MM in Eq. (1) increases by λ^2 with increasing wavelength λ, whereas the MM period d is approximately proportional to λ. Therefore, the condition of the single-order regime (1) becomes more rigid with increasing λ. Let us suppose that we need a high-resolution LMG operating at approximately λ = 13.5 nm, e.g., for metrology and monitoring of radiation sources used in an EUV lithography system [15]. The maximal reflectivity is achieved with Mo/Si MMs (approximately 74% for s-polarization in theory), the angular bandwidth of which is 4.98° at θ = 45° grazing incidence angle and thickness ratio $\gamma = d_{Mo}/d = 0.35$. The d-spacing of the MM is d=10 nm. Consequently, according to Eq. (1), the maximal possible lamel width is only 38.7 nm ("much less" means a factor of 3 here).

To date, the minimal lamel width achieved experimentally is 60 nm [13] and the aspect ratio (lamella height-to-width) is about 17. The fabrication of LMGs with smaller lamel widths is very difficult as the etching of such a grating structure can cause severe damage to the multilayer inside the lamels or even collapse of the lamellar structure. However, if we use $MoSi_2$/Si MMs with a lower optical contrast, the reflectivity bandwidth decreases to 2.27° (at γ = 0.4), the peak reflectivity also decreases to 54%, whereas the maximal possible lamel width increases to a practicable value of 82.9 nm. Therefore, we believe that the use of MM with low optical contrast is the only way to fabricate high-resolution LMGs with practical efficiency operating in the EUV region.

The choice of a material pair with low optical contrast is also important for the LMGs operating in the SXR spectral region. Let us consider the design of an LMG operating at approximately λ = 1 nm (E = 1.2 keV) with a high resolution (E/ΔE). The necessary number of bilayers should be $N_{LMG} \sim E/\Delta E$. The lamel height, being an additional crucial etching parameter, is equal to $h = N_{LMG}d$, thus being minimal for a small bilayer thickness d. Following [13], we set d = 2.5 nm and the thickness of the absorbing layer to 1 nm, assuming that the thickness is practicable for the deposition of smooth continuous films. Let us consider three LMGs based on W/Si, $MoSi_2$/Si, and SiC/Si MMs with different optical contrasts between the neighboring layers. We neglect the formation of interlayers for simplicity of analysis. Please note that the peak reflectivity of the MMs is 47%, 45%, and 34%, respectively. According to Eq. (1); the maximal possible lamel widths are approximately 156 nm, 366 nm, and 1110 nm for W/Si, $MoSi_2$/Si, and SiC/Si LMGs, respectively, while a factor of 5 for the "much less" value is needed here. Evidently, the wider the lamel, the easier it can be fabricated.

Assuming the achievable aspect ratio (i.e., the lamel height-to-width ratio) of A=17 [13], the number of bilayers of LMG should be approximately 1060, 2489, and 7548 for

W/Si, $MoSi_2$/Si, and SiC/Si MMs, respectively. We do not discuss here the detailed problems of the deposition and etch process of different material pairs. The mentioned values characterize the ultimate spectral resolution E/ΔE of 540, 1310, and 4470, respectively, which can be achieved with the corresponding LMGs. Therefore, if we need an LMG with an ultrahigh resolution exceeding e.g. 600, only MMs with low optical contrast can be used.

On the other hand, if MMs with low optical contrasts are used, the same resolution can be obtained with an essentially lower lamel aspect ratio, which significantly simplifies the LMG fabrication. Moreover, the diffraction efficiency of LMG with a larger lamel width is less sensitive to etching damages occurring on sidewalls [16]. A schematic of the low contrast LMG structure is shown in Fig. 1, characterized by the essentially larger lamel width (*ΓD*) that can satisfy the single-order condition compared to the high contrast LMG. The theoretical efficiency and required structures of the W/Si and $MoSi_2$/Si LMGs to achieve a same resolution of 540 are shown in Fig. 2. The grazing incident angle is around 11.95 °. For the W/Si LMG, the lamel width is 158 nm with a grating period of D=1216 nm and a large aspect ratio of A=17. For the $MoSi_2$/Si LMG, the lamel width is increased to 368 nm with a similar period of D=1170 nm and the aspect ratio is much smaller, A=7.3. The reflectance of W/Si and $MoSi_2$/Si MM is also shown as a comparison. These advantages make LMGs with low-optical-contrast materials more promising in terms of achieving high resolution and efficiency. In the present study, we demonstrate for the first time the feasible fabrication of a low-optical-contrast $MoSi_2$/Si LMG and characterize its performance in the SXR range.

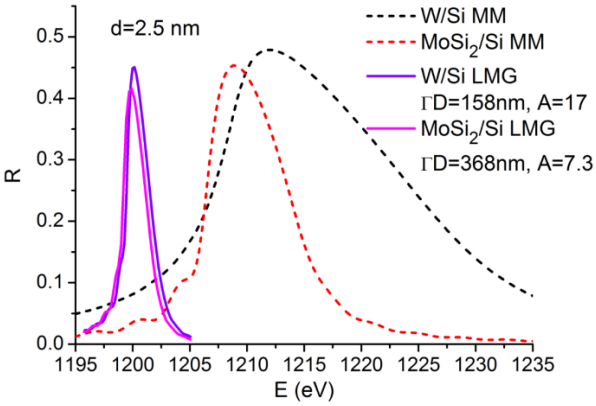

Fig. 2 Theoretical efficiency of the W/Si and MoSi2/Si LMGs with the maximal possible lamel widths and a same resolution of E/ΔE=540 at around 1200 eV. The reflectance of the two MMs is also shown. The d-spacings of all MLs are 2.5 nm.

2. Experimental results

A $MoSi_2$/Si LMG was designed with Γ = 1/3, D = 600 nm, and a lamel width of 200 nm. This relatively small lamel width was chosen to completely satisfy the single-order condition (1). The multilayer structure was designed with d_{Mo} = 2 nm and d_{Si} = 3 nm to guarantee good MM quality for the subsequent etching process. The number of MM bilayers N_{ML}= 60 is sufficient to obtain a reflectivity close to the maximal one at the photon energy of 1.2 keV. Thus, the bilayer number for the LMG was increased to NLMG = N_{ML}/Γ = 180 with a total thickness of h = 900 nm.

The multilayer was fabricated using the direct-current magnetron sputtering. The base pressure before the deposition was 9×10^{-5} Pa and the working pressure was 0.13 Pa with high-purity Ar. The deposition rates of $MoSi_2$ and Si were approximately 0.11 nm/s. The MM was deposited on super-polished Si wafers with a surface roughness below 0.2 nm. The fabricated MM was first characterized by grazing incidence X-ray reflectometry (GIXR) using the Cu-Kα line (E = 8.05 keV) in a lab-based X-ray diffractometer. Apart from the interface quality, the layer thickness drift over the MM stack is another critical factor decreasing the reflectance and broadening the reflectivity peak; in particular, that of a narrowband LMG [13]. To estimate the real multilayer structure, a two-layer model of $MoSi_2$/Si was used to fit the GIXR curve using the IMD software [17]. The thickness drifts of both $MoSi_2$ and Si layers were included in the model. As seen in Fig. 1, the fitted curve coincides well with the measured GIXR curve. The angular width of the high-order Bragg peaks, which are sensitive to the thickness drift over the MM stack, is also consistent with the measurement. According to the fitted results, the interface width (including roughness and diffusion) is approximately 0.32 nm, assuming an error function of the interface profile. The density of the Si layers is close to the bulk value (2.33 g/cm^3), and the density of the MoSi2 layers is approximately 87% of the bulk value (6.31 g/cm^3). A nonlinear drift of the MM period was estimated to be approximately 0.05 nm in the complete MM stack. This kind of thickness drift was also found in other works [18] and its effect will be further discussed later. The surface morphology of the multilayer was measured by atomic force microscopy (AFM) with a scanning area of $1\times1\mu m^2$. The roughness is very small, with a root-mean-square value of 0.17 nm. This is consistent with the relatively small interface width found above.

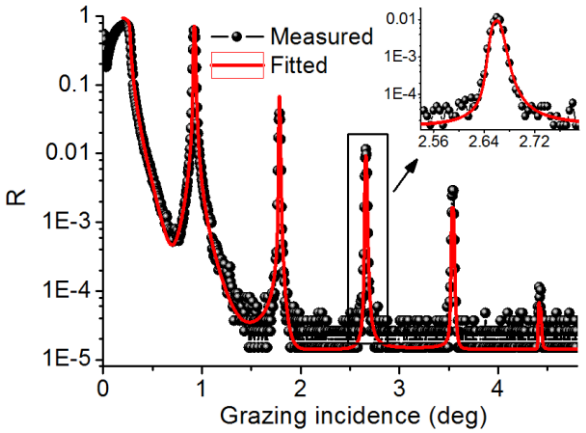

Fig. 3. Measured (circles) and fitted (solid curve) reflectivity at E = 8.05 keV of fabricated $MoSi_2$/Si MM with 180 bilayers. Inset: Enlarged 3rd order Bragg peak.

The LMG was fabricated using a combined process of electron beam lithography (EBL) and reactive ion etching. The grating pattern with a period of 600 nm was first defined via EBL in the resist coated on the MM surface. In the first

demonstration, the resist was directly used as the etching mask to etch the grating structure into the MM. To achieve a high aspect ratio of the LMG, the Bosch-type deep-etching technique was chosen using SF_6 and C_4F_8 as etching and passivation gases, respectively [19,20]. The etching process was optimized to obtain vertical sidewalls and to minimize damages in the multilayer. The etched grating structure was characterized via scanning electron microscopy (SEM) (Fig. 4). The period of the fabricated grating is D = 614 nm and the ratio of the lamel width to the grating period is Γ=~0.38. The etching depth is approximately 670 nm; i.e., approximately 45 bilayers at the bottom were not etched. This will cause a slight increase in the bandwidth and a loss in the reflectance compared with the fully etched LMG structure. The grating sidewalls are formed vertically which indicate a good directionality of the etching process. The nanoscale multilayer inside each lamel was studied using transmission electron microscopy (TEM). The TEM measurements were performed with FEI Talos equipment, and the sample was prepared by the focused ion beam technique. As shown in Fig. 5 the layers remained almost intact inside the lamel from the top surface to the bottom. The interfaces between $MoSi_2$ and Si layers are flat and sharp and the layers are in amorphous state according to the electron diffraction measurement (Fig. 5d). Only a small damaged area with a width of approximately 5 nm was found near the sidewalls (Fig. 5b). It is indicated that a good quality of the multilayer is preserved after etching.

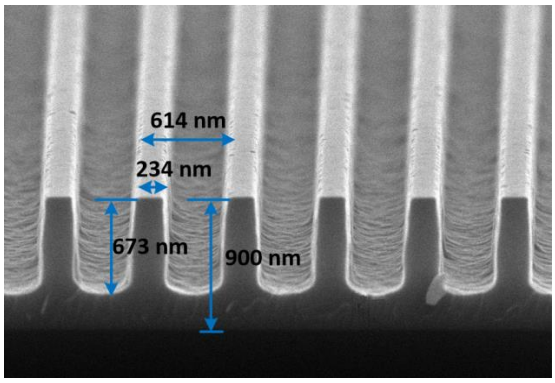

Fig. 4. An SEM image of the cross-section of the fabricated $MoSi_2$/Si LMG.

To study the SXR performance, both the MM and LMG were measured at the optics beamline of the BESSY-II synchrotron radiation facility [21]. A 1200 l/mm grating was used in the monochromator, providing an energy bandwidth of approximately 0.2 eV and a 0.13 angular divergence (full width at half maximum, FWHM) of the s-polarized beam at E =~1 keV. The unetched MM was first measured at grazing incidence angles of 8.4 °, 6.14 °, and 4.4 ° for different energy intervals (Fig. 6a, b, c). The experimental reflectance is 20%, 32%, and 45% at 881 eV, 1199 eV, and 1670 eV, respectively. The gradually increased reflectance is due to the lower absorption of $MoSi_2$ and Si at energies close to the Si-K edge (E = 1.83 keV). The fitting of the measured SXR reflectance results in almost the same parameters regarding those deduced from the HXR curve (Fig. 3). The measured spectral resolution of the MM is E/ΔE = 48–57 for 881–1670 eV. The parameters characterizing the theoretical and experimental SXR performance are listed in Table 1. The discrepancy between theoretical reflectance/bandwidth and the experimental values of the MM are caused by the interface roughness/diffusion and the slightly lower density of the layers compared to the bulk value.

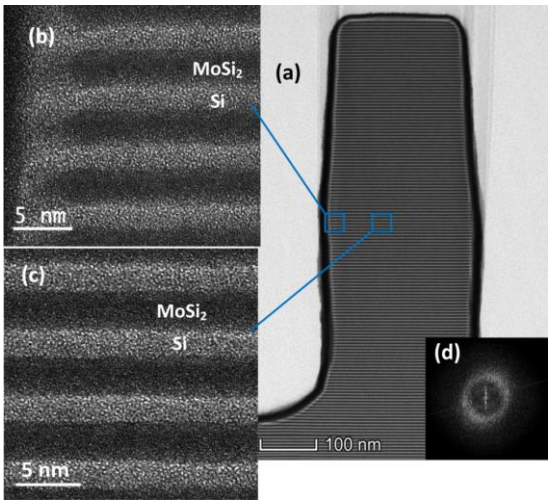

Fig. 5 TEM images of the etched grating lamel (a) and the multilayer strcutures inside the lamel (b, c). A electron diffracion pattern of the multilayer is shown in (d).

The 0th-order efficiency (reflectivity) of the fabricated LMG was measured at the same incidence angles to compare the results with those of the MM. High efficiencies of 16%, 26%, and 33% for 876 eV, 1183 eV, and 1648 eV were achieved, respectively (Fig. 6). The LMG reflectance reaches 80%–73% of the MM values. The shift in the peak position compared with that of the MM is caused by the different effective densities of the layers in the MM and LMG [11]. The energy bandwidths (FWHM) decreased to 8.3 eV (E = 876 eV), 11.0 eV (E = 1183 eV), and 16.1 eV (E = 1648 eV), which correspond to 45%–54% of the values of the initial MM. Thus, the spectral resolution is improved to E/ΔE=106–103 with a maximal enhancement factor of 2.2.

The dependence of the SXR efficiency on the grazing incidence angle was also measured at E = 1200 eV (Fig. 6d). The angular bandwidths of the MM and LMG are 0.116 ° and 0.056 °, respectively. Thus, the angular bandwidth reduction is approximately 2.1, as in the energy resolution. Considering the narrow angular bandwidth of the LMG, an angular accuracy of $< \pm 0.015$ ° is needed to maintain above 80% of the maximum 0th order efficiency and to select the exact photon energy. This brings a high requirement on the alignment accuracy for the application of such multilayer grating optics.

Given to the Γ ratio of 0.38, the resolution enhancement is expected to be $1/\Gamma = 2.6$. The discrepancy in the expected and measured bandwidths as well as the reflectance losses can be explained as follows: First, the 180 bilayers were not completely etched, which reduces the reflectance and broadens the reflectivity peak by an approximate factor of 1.09 according to simulations. The second reason is the

thickness drift inside the multilayer. The LMG has a smaller tolerance for thickness variations than the mirror owing to a smaller bandwidth [13]. The 50 pm drift of the d-spacing over the multilayer stack broadens the Bragg peak by a factor of ~1.14 and decreases the reflectance by ~5 rel.% compared with an ideal LMG without drift.

To compare the experimental and expected LMG performance in more detail, the SXR efficiency of the imperfect LMG was simulated. We assumed for simplicity that imperfections in the multilayer structure (interfacial roughness, possible oxygen and argon admixtures in layers) influence the MM and LMG reflectivity by the same manner. Therefore, we can introduce a reflectance factor (RF) as the ratio of the experimental peak reflectance of the MM to its theoretical value. The efficiency of the fabricated LMG was simulated using the structure parameters estimated from the SEM image and further decreasing them by the RF value. The simulation results are shown in Fig. 6a-c by dashed curves. They describe adequately the measured LMG efficiency including oscillations observed at the high-energy side of the peak. The oscillations are caused by the interference of waves reflected from the LMG and unetched MM underneath. The effect is more pronounced in the high-energy region, where the unetched MM reflectivity is high.

It is noteworthy that the calculated peak efficiency is still slightly higher than the measured ones in spite of the included imperfections of the MM. An additional efficiency loss can be explained by specific LMG imperfections caused during the grating structure fabrication, such as a damage of the multilayer structure induced by etching (in particular, near the lamel sidewalls) and deviations of the lamel shape from an ideal rectangle (Fig. 4). The effects of both factors on the LMG efficiency and resolution were analyzed in [16].

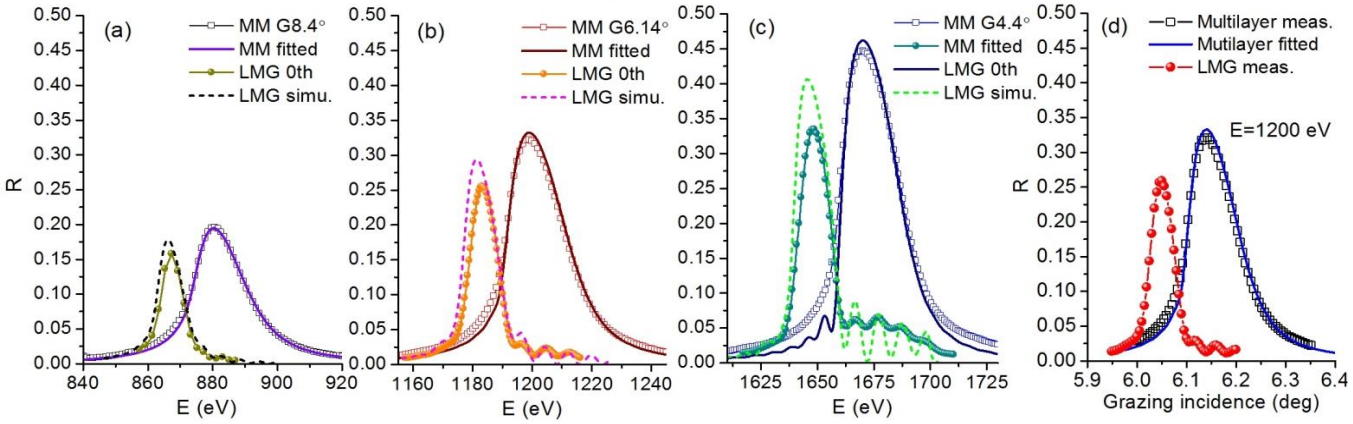

Fig. 6. Measured (symbols) and calculated (solid and dashed curves) SXR reflectivity of $MoSi_2$/Si MM and LMG versus photon energy at different grazing incidence angles of (a) 8.4 °, (b) 6.14 °, and (c) 4.4 °and (d) versus the grazing angle at E = 1200 eV.

Table 1 Parameters of the theoretical and measured SXR performance of the fabricated MM and LMG

	Grazing angle = 8.4 °				Grazing angle = 6.14 °				Grazing angle = 4.4 °			
	Efficiency	ΔE (eV)	E/ΔE	E (eV)	Efficiency	ΔE (eV)	E/ΔE	E (eV)	Efficiency	ΔE (eV)	E/ΔE	E (eV)
MM theo.*	28%	21.7	41	881	44%	27.5	44	1200	60%	37.1	45	1670
MM expe.	20%	18.5	48	881	32%	22.5	53	1199	45%	29.5	57	1670
LMG theo.**	26%	9.2	94	865	41%	12.2	97	1181	55%	18.8	88	1644
LMG expe.	16%	8.3	106	867	26%	11.0	108	1183	33%	16.1	103	1648

*The theoreical efficiency of MM is calculated with the ideal structure. **The theoretical effiicency of LMG is calculated with the grating profile obtained from SEM images and the ideal multilayer structure.

3. Summary

It has been theoretically showed that high efficiency and high resolution LMGs operating in the SXR/EUV region can only be realized with low optical contrast materials composing the multilayer structure. For a first demonstration, a $MoSi_2$/Si MM (d = 5 nm, N = 180) was deposited using magnetron sputtering. The Bosch-type deep-etching process was optimized for the fabrication of the grating structure and minimizing layer damages. The SXR measurements exhibit a high reflectivity (0th-order diffraction efficiency) of the LMG, achieving 16%–33% for 876 eV–1648 eV, i.e., 73%–80% of the reflectance of the unpatterned MM. The resolution of the LMG exceeds 100 with a maximal increase factor of 2.2, compared with the conventional MM. The experimental values are rather close to the theoretical ones. Further improvements in the $MoSi_2$/Si LMG include reducing the multilayer period to 2.5 nm, increasing the etching depth and lamel width to the maximal theoretical

value that satisfies the single-order operation regime, and decreasing the period drift in the MM. These will be investigated in the future studies.

Acknowledgements

This work is supported by National Natural Science Foundation of China (NSFC) (Nos. 61621001, 11505129, U1732268, 11443007), National Key R&D Program of China (Nos. 2016YFA0401304, 2017YFA0403302). Russian Ministry of Science and Higher Education within the State assignment FSRC "Crystallography and Photonics" RAS.

References

1. Mimura H, Handa S, Kimura T, et al., 2010 Nat. Phys. **6**, 122.
2. Wagner C and Harned N, 2010 Nat. Photonics, **4**, 24.
3. Senf F, Bijkerk F, Eggenstein F et al., 2016 Opt. Express **24**(12), 13220.
4. Voronov D L, Gullikson E M, Salmassi F et al., 2014 Opt. Lett. **39**(11), 3157.
5. Huang Q, Medvedev V, Van de Kruijs R, et al., 2017 Appl. Phys. Rev. **4**, 011104.
6. Bajt S, Prasciolu M, Hamm C E, at al., 2018 Light: Sci. Appl. **7**, 17162.
7. Jonnard P, Le Guen K, Andr é J M. et al., 2012 X-Ray Spectrom. 41, 308.
8. Duorah S, Ejiri A, Lee S, et al., 2001 Rev. Sci. Instrum. **72**(1), 1183.
9. Andr é J M, Benbalagh R, Barchewitz R et al., 2002 Appl. Opt. **41**(1), 239.
10. Martynov V V and Platonov Yu, 2002 Rev. Sci. Instrum. **73**(3), 1551.
11. Kozhevnikov I V, Van der Meer R, Bastiaens H J M et al., 2010 Opt. Express **18**, 16234.
12. Kozhevnikov I V, Van der Meer R, Bastiaens H M J, et al., 2011 Opt. Express **19**, 9172.
13. Van der Meer R, Kozhevnikov I, Krishnan B et al., 2013 AIP Adv. **3**, 012103.
14. Kozhevnikov I V and Vinogradov A V, 1987 Phys. Scr. **T17**, 137.
15. Barreaux J L P, Kozhevnikov I V, Bayraktar M, et al., 2017 Opt. Express **25**, 1993.
16 Van der Meer R, Kozhevnikov I V, Bastiaens H M J, et al., 2013 Opt. Express **21**, 13105.
17. Windt D L, 1998 Comput. Phys. **12**, 360.
18 Huang Q, Li H, Zhu J, Wang Z and Chen H, 2013, J. Phys. D: Appl. Phys. **46** 275105.
19. Woldering L A, Tjerkstra R W, Jansen H V et al., 2008 Nanotechnology **19**, 145304.
20. Van der Meer R, Krishnan B, Kozhevnikov I V, et al., 2011 Proc. SPIE **8139**, 81390Q.
21. Sokolov A, Bischoff P, Eggenstein F, et al., 2016 Rev. Sci. Instrum. **87**, 052005.